



HAL
open science

Epitaxial Heusler alloy Co_2FeSi films on Si(111) substrates grown by molecular beam epitaxy

M Zander, J Herfort, K Kumakura, H.-P Schönherr, A Trampert

► **To cite this version:**

M Zander, J Herfort, K Kumakura, H.-P Schönherr, A Trampert. Epitaxial Heusler alloy Co_2FeSi films on Si(111) substrates grown by molecular beam epitaxy. *Journal of Physics D: Applied Physics*, 2010, 43 (30), pp.305004. 10.1088/0022-3727/43/30/305004 . hal-00569660

HAL Id: hal-00569660

<https://hal.science/hal-00569660>

Submitted on 25 Feb 2011

HAL is a multi-disciplinary open access archive for the deposit and dissemination of scientific research documents, whether they are published or not. The documents may come from teaching and research institutions in France or abroad, or from public or private research centers.

L'archive ouverte pluridisciplinaire **HAL**, est destinée au dépôt et à la diffusion de documents scientifiques de niveau recherche, publiés ou non, émanant des établissements d'enseignement et de recherche français ou étrangers, des laboratoires publics ou privés.

Epitaxial Heusler alloy Co_2FeSi films on Si(111) substrates grown by molecular beam epitaxy

M. Zander^{a)}, J. Herfort, K. Kumakura^{b)}, H.-P. Schönherr, and A. Trampert

*Paul-Drude-Institut für Festkörperelektronik,
Hausvogteiplatz 5–7, 10117 Berlin, Germany*

Abstract

The influence of growth temperature on the structural and magnetic properties of Heusler alloy Co_2FeSi films grown on Si(111) substrates has been studied. Reflection high energy diffraction (RHEED), double crystal x-ray diffraction (DCXRD) and transmission electron microscopy (TEM) measurements revealed that Co_2FeSi layers were epitaxially grown on Si(111) substrates in an optimized growth temperature range $150\text{ }^\circ\text{C} < T_G < 200\text{ }^\circ\text{C}$. From double crystal x-ray diffraction measurements and transmission electron microscopy, it was shown that in the optimized temperature range the $\text{Co}_2\text{FeSi}/\text{Si}(111)$ films crystallize in the $B2 + L2_1$ structures. All layers are ferromagnetic and well-ordered films on Si(111) show high magnetic moments with an average value of $(1140 \pm 250)\text{ emu/cm}^3$, which is in good agreement with the value of bulk Co_2FeSi at 300 K. The magnetic anisotropy is correlated to the structural properties of the layers.

PACS numbers: 68.35.Ct, 75.50.Cc, 81.15.Hi

^{a)} Electronic mail: marlenezander@moegei.waseda.jp

^{b)} Permanent address: NTT Basic Research Laboratories, 3-1 Morinosato Wakamiya, Atsugi-shi, Kanagawa 243-0198, Japan.

I. INTRODUCTION

Spintronic devices are making use of the spin degree of freedom of the electron and are expected to offer new perspectives to semiconductor device technology. One of the key issues for the realization of spintronic devices is the efficient electrical injection of spin-polarized carriers into semiconductors. Therefore, epitaxial ferromagnet/semiconductor (FM/SC) heterostructures have attracted considerable attention. In particular, Heusler alloys are promising candidates for a spin injection source into semiconductors, because of their high Curie temperature and half-metallicity predicted for some Heusler alloys.¹⁻⁵ To date, mainly the fabrication of ferromagnetic Heusler alloy/III-V semiconductor hybrid structures has been reported.⁶⁻¹⁰ On the other hand, there have been so far only few attempts to grow ferromagnetic Heusler alloys on group-IV semiconductors,¹¹⁻¹³ despite the fact that these semiconductors are important for an integration of spintronic devices into Si large-scale integrated circuits. In addition to its importance in electronics, Si is a highly attractive semiconductor for spintronic devices due to an enhanced spin relaxation time and a large transport length of the electrons.¹⁴ Only recently, spin injection into Si was demonstrated.^{15,16} In the past, growth of binary Heusler alloy Fe₃Si on Si substrates was reported and the electrical injection and detection of spin-polarized electrons into Si through an Fe₃Si/Si Schottky tunnel barrier was shown.^{12,16} However, Fe₃Si does not exhibit 100% spin polarization at the Fermi level.

Co₂FeSi is one member of full-Heusler alloys with the cubic $L2_1$ crystal structure. The $L2_1$ structure can be considered as four interpenetrating fcc sublattices A, B, C, and D with origins at (0 0 0), (1/4 1/4 1/4), (1/2 1/2 1/2), and (3/4 3/4 3/4).¹⁷ The A and C sublattices are occupied by Co, and the B and D sublattices by Fe and Si, respectively. The atomically ordered $L2_1$ structure is reduced to the $B2$ (CsCl) structure, when the Fe(B) and Si(D) sublattices are completely disordered. The lattice constant of bulk Co₂FeSi is 5.658 Å,¹⁸ and has a lattice mismatch of 4% relative to the Si(001) substrate. Bulk Co₂FeSi with a large magnetic moment ($\approx 6 \mu_B$)^{5,18} is ferromagnetic up to more than 1100 K.⁵ In addition, Co₂FeSi is expected to exhibit halfmetallic behaviour.⁵ Recently, electrical spin injection from an epitaxial Co₂FeSi thin film into GaAs was demonstrated.¹⁹ For an effective injection of spin polarized electrons into the semiconductor the quality of the Co₂FeSi layer at the ferromagnetic/semiconductor interface is crucial. Therefore, one requirement for successfully using Co₂FeSi as a spin injection source into the semiconductor is the defined (preferably epitaxial) growth of thin films with high crystal quality at the interface. In this study, therefore,

the structural and magnetic properties of Heusler alloy Co_2FeSi films grown on Si(111) substrates grown by molecular beam epitaxy (MBE) at different temperatures T_G were investigated. For the structural characterization, reflection high energy electron diffraction (RHEED), atomic force microscopy (AFM), x-ray diffractometrie (XRD), x-ray reflectometry (XRR) and transmission electron microscopy (TEM) were used. The magnetic properties were investigated with a SQUID (superconducting quantum interference device) system.

II. EXPERIMENTAL

The growth is initiated on a Si(111)-(7×7) reconstructed surface for providing well-defined surface conditions. To deoxidize the substrates prior to the growth two different deoxidation methods have been used. The first growth study of Co_2FeSi films was carried out on *in-situ* deoxidized substrates. The Si substrates were treated with Ga for one minute at a substrate temperature $T_S = 500$ °C and than heated for 5 minutes at $T_S = 700$ °C. After the treatment Si(111)-(7×7) reconstruction pattern were observed by reflection high energy electron diffraction (RHEED). However, AFM measurements revealed some contamination with particles on the surface most likely connected to the deposition of Ga atoms. To avoid a possible contamination with Ga, for later growth studies the Si substrates were ex-situ deoxidized using 10% hydroflouric acid followed by 5 minutes *in-situ* heating at $T_S = 650$ °C in the MBE growth chamber. The wet chemical treatment resulted in a smoother surface with atomic steps prior to the growth (root-mean-square roughness ≈ 0.3 nm) as evidenced via AFM measurements.

Co, Fe and Si are than codeposited from high-temperature effusion cells at substrate temperatures varied between 100 and 300 °C, at a growth rate of 0.1 nm/min with a base pressure of 1×10^{-10} Torr. The evaporation rates are controlled by the cell temperatures and are in accordance with the optimized fluxes for the growth of stoichiometric Co_2FeSi films on GaAs(001) substrates.²⁰ The thickness of the layers is between 15 and 42 nm as determined by x-ray reflectivity measurements.

III. RESULTS AND DISCUSSION

The growth was monitored *in-situ* using reflection high energy electron diffraction (RHEED). For substrate temperatures $T_G \leq 200$ °C, after 1-3 monolayer of growth streaky pattern are ob-

served implying the formation of smooth Co_2FeSi layers on the $\text{Si}(111)$ substrate (not shown here). The observed RHEED pattern is symmetric for electron beam direction along the $\text{Si} [11\bar{2}]$ azimuth and for any multiple of 60° . An identical RHEED pattern is seen every 120° . From the analysis of the RHEED pattern it was found that $(111)\text{Co}_2\text{FeSi}||(\text{111})\text{Si}$, giving a first evidence that epitaxial grown films are obtained. For samples with $T_G \geq 250^\circ\text{C}$ we observed spotty RHEED pattern after 3 ML of growth implying the formation of three-dimensional structures at the interface. We note here that attempts to growth epitaxial Co_2FeSi films on $\text{Si}(001)$ lead to polycrystalline grains only as evidenced by RHEED and DCXRD measurements.²¹

Figure 1 shows double crystal x-ray diffraction (DCXRD) $\omega - 2\theta$ scans measured with an open detector ranging from $\text{Si}(111)$ to $\text{Si}(222)$ reflections for different T_G . Pronounced peaks due to the $\text{Co}_2\text{FeSi}(222)$ layer reflection were only obtained in a relatively narrow temperature range between $T_G = 150$ and 200°C . At higher T_G , strong interfacial reactions set in, which are derived from the observation of the $\text{FeSi}(210)$ and $\text{CoSi}_2(222)$ reflections for the films grown at $T_G = 250$ and 300°C , respectively. This is in good agreement with the observation of spotty RHEED pattern for samples with $T_G \geq 250^\circ\text{C}$. In addition, atomic force microscopy measurements showed a strong degradation of the surface for $T_G \geq 210^\circ\text{C}$ with a root mean square (rms) roughness ≥ 3 nm, where for well-ordered films with $150^\circ\text{C} < T_G < 200^\circ\text{C}$ a rms-roughness of (0.4 ± 0.1) nm was found. For $T_G \leq 120^\circ\text{C}$, no diffraction peak of the layer could be observed, which indicates the absence of a structural order of the Heusler alloy. The measured difference between the $\text{Co}_2\text{FeSi}(222)$ and $\text{Si}(222)$ reflections is $\Delta\theta_B \approx 1.43^\circ$ which is smaller than the theoretical difference of 1.6° for a fully strained layer, indicating that the layers are partially relaxed. This also explains the absence of fringes in the $\omega - 2\theta$ scans despite the smooth surface of the films, which is different to the case of Co_2FeSi films on $\text{GaAs}(001)$ substrates.²⁰ In addition, the appearance of the $\text{Co}_2\text{FeSi}(222)$ reflection suggests that at least the $B2$ structure is formed implying a spin polarization in the grown film. However, for the confirmation of the $L2_1$ structure, which is required to obtain 100% spin polarization in the film, additional reflections with all odd Miller indices like the $\text{Co}_2\text{FeSi}(111)$ reflection need to be observed. Figure 2 compares DCXRD $\omega - 2\theta$ scans measured with an open detector ranging from $\text{Si}(111)$ to $\text{Si}(222)$ reflections for films grown at $T_G = 160^\circ\text{C}$ with $d \approx 16$ nm and $d \approx 42$ nm, respectively. For the 16 nm thick film only a weak shoulder peak due to the $\text{Co}_2\text{FeSi}(111)$ reflection is observed. However, for the 42 nm thick sample the $\text{Co}_2\text{FeSi}(111)$ peak as well as the $\text{Co}_2\text{FeSi}(222)$ peak are clearly more pronounced indicating an ordering in the $L2_1$ structure. The pronounced observation of the $\text{Co}_2\text{FeSi}(111)$ reflection in thicker films can be

either due to the enhanced intensity of the reflection and/or a thickness dependent improvement of the long-range atomic ordering as observed in Co_2FeSi films on $\text{GaAs}(001)$ substrates.¹⁰

The crystallinity and interface properties were investigated using cross-sectional transmission electron microscopy (TEM). Figure 3 (a) shows a high-resolution TEM (HRTEM) image along the $\text{Si}-[11\bar{2}]$ zone axis for the well-ordered film grown at $T_G = 160^\circ\text{C}$ with $d \approx 42$ nm near the $\text{Co}_2\text{FeSi}/\text{Si}(111)$ interface. Despite the lattice mismatch, a very sharp $\text{Co}_2\text{FeSi}/\text{Si}(111)$ interface and an atomic scale abruptness could be obtained. This is more clearly seen in Figure 3 (b) where the noise-reduced (Fourier-filtered) enlarged HRTEM image of the interface is shown. In Figure 3 (c) a nanobeam diffraction pattern of the Co_2FeSi layer near the Si interface is presented. From the observation of the two brighter areas on the $\text{Co}_2\text{FeSi}(222)$ reflection, which is due to an overlap of the $\text{Co}_2\text{FeSi}(111)$ and (333) reflection with the (222) reflection, the existence of the ordered $L2_1$ phase is derived. Furthermore, Co_2FeSi grows epitaxially on $\text{Si}(111)$ with $(111)\text{Co}_2\text{FeSi}|| (111)\text{Si}$, which is derived from the analysis of the diffraction pattern and is in good agreement with the RHEED and XRD measurements. In the HRTEM image [Fig. 3 (a)] additionally, relatively strong differences in brightness can be seen. As the lattice mismatch between the Co_2FeSi layer and the Si substrate is relatively large, the contrast differences at the interface are most likely due to local strain variations. From the HRTEM images the existence of a few misfit dislocations was found (not shown here), which explains the partial relaxation of the Co_2FeSi layer as observed by XRD measurements. For the sample with $T_G = 200^\circ\text{C}$ TEM measurements revealed the existence of an interlayer at the interface (not shown here) which is explained by the initiation of interfacial reactions at this temperature. A strong degradation of the ferromagnet/semiconductor interface was found for $T_G \geq 210^\circ\text{C}$.

The magnetic properties of the layers were measured using superconducting quantum interference device magnetometry (SQUID) at 300 K. Figure 4 shows the hysteresis loop for the sample with $T_G = 160^\circ\text{C}$ and $d \approx 42$ nm.

The external magnetic field was applied along the $[11\bar{2}]$ and $[1\bar{1}0]$ directions. The layer is ferromagnetic at room temperature, where the relatively easy axis of magnetization is in the film plane along the $[11\bar{2}]$ direction and the hard axis along the $[1\bar{1}0]$ direction, indicating the presence of an uniaxial magnetic anisotropy in the film plane. This is in good agreement with the investigation of $\text{Co}_2\text{FeSi}/\text{GaAs}(001)$ hybrid structures.²⁰ Ando *et al.* recently showed an uniaxial magnetic anisotropy in Fe_3Si films on $\text{Ge}(111)$, where the magnetic easy axis is oriented randomly for each of the samples.¹³ For the Co_2FeSi films on $\text{Si}(111)$ it was found that the relatively easy axis was

oriented along the $[11\bar{2}]$ direction for all films. The presence of an uniaxial magnetic anisotropy is most likely correlated with the high crystal quality of the Co_2FeSi layer at the interface.²² The coercive fields $H_C = 10 - 20$ Oe are rather small for all examined orientations, but are higher than in the case of Co_2FeSi layers on $\text{GaAs}(001)$, which is explained by the existence of defects pinning magnetic domains.²³ For well-ordered Co_2FeSi films on $\text{Si}(111)$ with $150^\circ\text{C} < T_G < 200^\circ\text{C}$ the magnetic moment at the saturation magnetization is almost constant within the error limit as seen in figure 5.

The average magnetic moment for these films amounts to (1140 ± 250) emu/cm³, which is close to the bulk value of Co_2FeSi .^{5,18} For higher $T_G \geq 210^\circ\text{C}$ the magnetic moment is decreased implying the formation of magnetic modified compounds due to interfacial reactions in agreement with the results of the XRD, AFM and TEM measurements. Furthermore, the dependence on the measuring temperature T_{Meas} changes drastically with T_G . For $T_G \geq 210^\circ\text{C}$ the saturation magnetization measured at room temperature ($T_{Meas} = 300$ K) of the ferromagnetic layers is clearly decreased in respect to M_S at $T_{Meas} = 10$ K. This indicates the formation of magnetic modified compounds and/or phases at higher T_G .

IV. CONCLUSION

The MBE growth of thin ferromagnetic Co_2FeSi films on $\text{Si}(111)$ substrates at different growth temperatures T_G was studied. Epitaxial and well-ordered Co_2FeSi layers could be obtained on $\text{Si}(111)$ in an optimized temperature range $150^\circ\text{C} < T_G < 200^\circ\text{C}$. At $T_G = 160$ and 180°C layers in the $L2_1$ structure were realized. Well-ordered films show high magnetic moments with an average value of (1140 ± 250) emu/cm³, which is in good agreement with the value of bulk Co_2FeSi at 300 K. The results are promising for the application of $\text{Co}_2\text{FeSi}/\text{Si}(111)$ hybrid structures for future spintronic devices.

The research presented here was partly supported by the German BMBF under the research program NanoQUIT (Contract No. 01BM463). The authors would like to thank B. Jenichen, L. Geelhaar, and H. Riechert for useful discussions and B. Jenichen for a careful reading of the manuscript.

-
- ¹ R. A. de Groot, F. M. Mueller, P. G. van Engen, and K. H. J. Buschow, Phys. Rev. Lett. **50**, 2024 (1983).
- ² S. Fujii, S. Sugimura, S. Ishida, and S. Asano, J. Phys.: Condens. Matter **2**, 8583 (1990).
- ³ I. Galanakis, P. H. Dederichs, and N. Papanikolaou, Phys. Rev. B **66**, 174429 (2002).
- ⁴ C. Palmstrom, MRS Bull. **28**, 725 (2003).
- ⁵ S. Wurmehl, G. H. Fecher, H. C. Kandpal, V. Ksenofontov, C. Felser, H. J. Lin, and J. Morais, Phys. Rev. B **72**, 184434 (2005).
- ⁶ T. Ambrose, J. J. Krebs, and G. A. Prinz, Appl. Phys. Lett. **76**, 3280 (2000).
- ⁷ J. Lu, J. W. Dong, J. Q. Xie, S. McKernan, C. J. Palmstrom, and Y. Xin, Appl. Phys. Lett. **83**, 2393 (2003).
- ⁸ Y. J. Chen, D. Basiaga, J. R. O'Brien, and D. Heiman, Appl. Phys. Lett. **84**, 4301 (2004).
- ⁹ W. H. Wang, M. Przybylski, W. Kuch, L. I. Chelaru, J. Wang, Y. F. Lu, J. Barthel, H. L. Meyerheim, and J. Kirschner, Phys. Rev. B **71**, 144416 (2005).
- ¹⁰ M. Hashimoto, A. Trampert, J. Herfort, and K. H. Ploog, J. Vac. Sci. Techn. **25**, 1453 (2007).
- ¹¹ T. Sadoh, M. Kumano, R. Kizuka, K. Ueda, K. Kenjo, and M. Miyao, Appl. Phys. Lett. **89**, 182511 (2006).
- ¹² K. Hamaya, K. Ueda, Y. Kishi, Y. Ando, T. Sadoh, and M. Miyao, Appl. Phys. Lett. **93**, 132117 (2008).
- ¹³ Y. Ando, K. Hamaya, K. Kasahara, K. Ueda, Y. Nozaki, T. Sadoh, Y. Maeda, K. Matsuyama, and M. Miyao, J. Appl. Phys. **105**, 07B102 (2009).
- ¹⁴ I. Appelbaum, B. Q. Huang, and D. J. Monsma, Nature **447**, 295-298 (2007).
- ¹⁵ B. T. Jonker, G. Kioseoglou, A. T. Hanbicki, C. H. Li, and P. E. Thompson, Nature Phys. **3**, 542-546 (2007).
- ¹⁶ Y. Ando, Y. Hamaya, K. Kasahara, Y. Kishi, K. Ueda, K. Sawano, T. Sadoh, and M. Miyao, Appl. Phys. Lett. **94**, 182105 (2009).
- ¹⁷ For the details of $L2_1$ structure, see P. J. Webster and K. R. A. Ziebeck, *Landolt-Börnstein New Series III/19c*, (Springer, Berlin, 1988), p.75.
- ¹⁸ V. Niculescu T. J. Burch, K. Raj, and J. I. Budnick, J. Magn. Mater. **5**, 60-66 (1977).
- ¹⁹ M. Ramsteiner, O. Brandt, T. Flissikowski, H. Grahn, H. T. Hashimoto, J. Herfort, and H. Kostial, Phys. Rev. B **78**, 121303 (2008).
- ²⁰ M. Hashimoto, J. Herfort, H.-P. Schönherr, and K. H. Ploog, Appl. Phys. Lett. **87**, 102506 (2005).

- ²¹ M. Zander, H.-P. Schönherr, and J. Herfort, unpublished.
- ²² M. Hashimoto, J. Herfort, A. Trampert, and K. H. Ploog, *J. Cryst. Growth.* **301**, 592 (2007).
- ²³ J. Herfort, H.-P. Schönherr, K.-J. Friedland, and K. H. Ploog, *J. Vac. Sci. Technol. B* **22**, 2073 (2004).
- ²⁴ K. Ueda, R. Kizuka, H. Takeuchi, A. Kenjo, T. Sadoh, and M. Miyao, *Thin Sol. Films* **515**, 8250 (2007).

Figure captions

FIG. 1: DCXRD curves of the symmetric (111) and (222) reflections for different values of T_G . For samples grown between $T_G = 150$ and 200 °C, $\text{Co}_2\text{FeSi}(222)$ reflections are observed. For films grown at $T_G \geq 250$ °C, interfacial reactions set in. The thickness of the films is $d \approx 18$ nm.

FIG. 2: DCXRD curves of the symmetric (111) and (222) reflections for two different values of d at $T_G = 160$ °C. The appearance of the $\text{Co}_2\text{FeSi}(111)$ reflection indicates that an ordering in the $L2_1$ structure could be obtained.

FIG. 3: (a) A cross-sectional high-resolution TEM image of the Co_2FeSi film grown at $T_G = 160$ °C with $d \approx 42$ nm along the $\text{Si}-[11\bar{2}]$ zone axis. (b) Noise-reduced (Fourier-filtered) HRTEM image of the interface. The white triangles mark the position of the interface. (c) Nanobeam diffraction pattern of the epitaxial Co_2FeSi layer. The $\text{Co}_2\text{FeSi}(222)$ reflection is overlapped by the $\text{Co}_2\text{FeSi}(111)$ and (333) reflection.

FIG. 4: The magnetization curves of a Co_2FeSi film grown at $T_G = 160$ °C with $d \approx 42$ nm. The external magnetic field was applied along the $[11\bar{2}]$ and $[1\bar{1}0]$ axis. The diamagnetic contribution of the substrate has been subtracted.

FIG. 5: Saturation magnetization of the Co_2FeSi layers in dependence of T_G measured at $T_{Meas} = 10$ K. The external magnetic field was applied along the $[11\bar{2}]$ axis. For well-ordered Co_2FeSi films on $\text{Si}(111)$ with 150 °C $< T_G < 200$ °C the magnetic moment at the saturation magnetization is almost constant within the error limit.

-
- ¹ R. A. de Groot, F. M. Mueller, P. G. van Engen, and K. H. J. Buschow, *Phys. Rev. Lett.* **50**, 2024 (1983).
 - ² S. Fujii, S. Sugimura, S. Ishida, and S. Asano, *J. Phys.: Condens. Matter* **2**, 8583 (1990).
 - ³ I. Galanakis, P. H. Dederichs, and N. Papanikolaou, *Phys. Rev. B* **66**, 174429 (2002).
 - ⁴ C. Palmstrom, *MRS Bull.* **28**, 725 (2003).
 - ⁵ S. Wurmehl, G. H. Fecher, H. C. Kandpal, V. Ksenofontov, C. Felser, H. J. Lin, and J. Morais, *Phys. Rev. B* **72**, 184434 (2005).
 - ⁶ T. Ambrose, J. J. Krebs, and G. A. Prinz, *Appl. Phys. Lett.* **76**, 3280 (2000).
 - ⁷ J. Lu, J. W. Dong, J. Q. Xie, S. McKernan, C. J. Palmstrom, and Y. Xin, *Appl. Phys. Lett.* **83**, 2393 (2003).
 - ⁸ Y. J. Chen, D. Basiaga, J. R. O'Brien, and D. Heiman, *Appl. Phys. Lett.* **84**, 4301 (2004).
 - ⁹ W. H. Wang, M. Przybylski, W. Kuch, L. I. Chelaru, J. Wang, Y. F. Lu, J. Barthel, H. L. Meyerheim, and J. Kirschner, *Phys. Rev. B* **71**, 144416 (2005).
 - ¹⁰ M. Hashimoto, A. Trampert, J. Herfort, and K. H. Ploog, *J. Vac. Sci. Techn.* **25**, 1453 (2007).
 - ¹¹ T. Sadoh, M. Kumano, R. Kizuka, K. Ueda, K. Kenjo, and M. Miyao, *Appl. Phys. Lett.* **89**, 182511 (2006).
 - ¹² K. Hamaya, K. Ueda, Y. Kishi, Y. Ando, T. Sadoh, and M. Miyao, *Appl. Phys. Lett.* **93**, 132117 (2008).
 - ¹³ Y. Ando, K. Hamaya, K. Kasahara, K. Ueda, Y. Nozaki, T. Sadoh, Y. Maeda, K. Matsuyama, and M. Miyao, *J. Appl. Phys.* **105**, 07B102 (2009).
 - ¹⁴ I. Appelbaum, B. Q. Huang, and D. J. Monsma, *Nature* **447**, 295-298 (2007).
 - ¹⁵ B. T. Jonker, G. Kioseoglou, A. T. Hanbicki, C. H. Li, and P. E. Thompson, *Nature Phys.* **3**, 542-546 (2007).
 - ¹⁶ Y. Ando, Y. Hamaya, K. Kasahara, Y. Kishi, K. Ueda, K. Sawano, T. Sadoh, and M. Miyao, *Appl. Phys. Lett.* **94**, 182105 (2009).
 - ¹⁷ For the details of $L2_1$ structure, see P. J. Webster and K. R. A. Ziebeck, *Landolt-Börnstein New Series III/19c*, (Springer, Berlin, 1988), p.75.
 - ¹⁸ V. Niculescu T. J. Burch, K. Raj, and J. I. Budnick, *J. Magn. Magn. Mater.* **5**, 60-66 (1977).
 - ¹⁹ M. Ramsteiner, O. Brandt, T. Flissikowski, H. Grahn, H. T. Hashimoto, J. Herfort, and H. Kostial, *Phys. Rev. B* **78**, 121303 (2008).
 - ²⁰ M. Hashimoto, J. Herfort, H.-P. Schönherr, and K. H. Ploog, *Appl. Phys. Lett.* **87**, 102506 (2005).

- ²¹ M. Zander, H.-P. Schönherr, and J. Herfort, unpublished.
- ²² M. Hashimoto, J. Herfort, A. Trampert, and K. H. Ploog, *J. Cryst. Growth.* **301**, 592 (2007).
- ²³ J. Herfort, H.-P. Schönherr, K.-J. Friedland, and K. H. Ploog, *J. Vac. Sci. Technol. B* **22**, 2073 (2004).
- ²⁴ K. Ueda, R. Kizuka, H. Takeuchi, A. Kenjo, T. Sadoh, and M. Miyao, *Thin Sol. Films* **515**, 8250 (2007).

Figure captions

FIG. 1: DCXRD curves of the symmetric (111) and (222) reflections for different values of T_G . For samples grown between $T_G = 150$ and 200 °C, $\text{Co}_2\text{FeSi}(222)$ reflections are observed. For films grown at $T_G \geq 250$ °C, interfacial reactions set in. The thickness of the films is $d \approx 18$ nm.

FIG. 2: DCXRD curves of the symmetric (111) and (222) reflections for two different values of d at $T_G = 160$ °C. The appearance of the $\text{Co}_2\text{FeSi}(111)$ reflection indicates that an ordering in the $L2_1$ structure could be obtained.

FIG. 3: (a) A cross-sectional high-resolution TEM image of the Co_2FeSi film grown at $T_G = 160$ °C with $d \approx 42$ nm along the $\text{Si}-[11\bar{2}]$ zone axis. (b) Noise-reduced (Fourier-filtered) HRTEM image of the interface. The white triangles mark the position of the interface. (c) Nanobeam diffraction pattern of the epitaxial Co_2FeSi layer. The $\text{Co}_2\text{FeSi}(222)$ reflection is overlapped by the $\text{Co}_2\text{FeSi}(111)$ and (333) reflection.

FIG. 4: The magnetization curves of a Co_2FeSi film grown at $T_G = 160$ °C with $d \approx 42$ nm. The external magnetic field was applied along the $[11\bar{2}]$ and $[1\bar{1}0]$ axis. The diamagnetic contribution of the substrate has been subtracted.

FIG. 5: Saturation magnetization of the Co_2FeSi layers in dependence of T_G measured at $T_{Meas} = 10$ K. The external magnetic field was applied along the $[11\bar{2}]$ axis. For well-ordered Co_2FeSi films on $\text{Si}(111)$ with 150 °C $< T_G < 200$ °C the magnetic moment at the saturation magnetization is almost constant within the error limit.

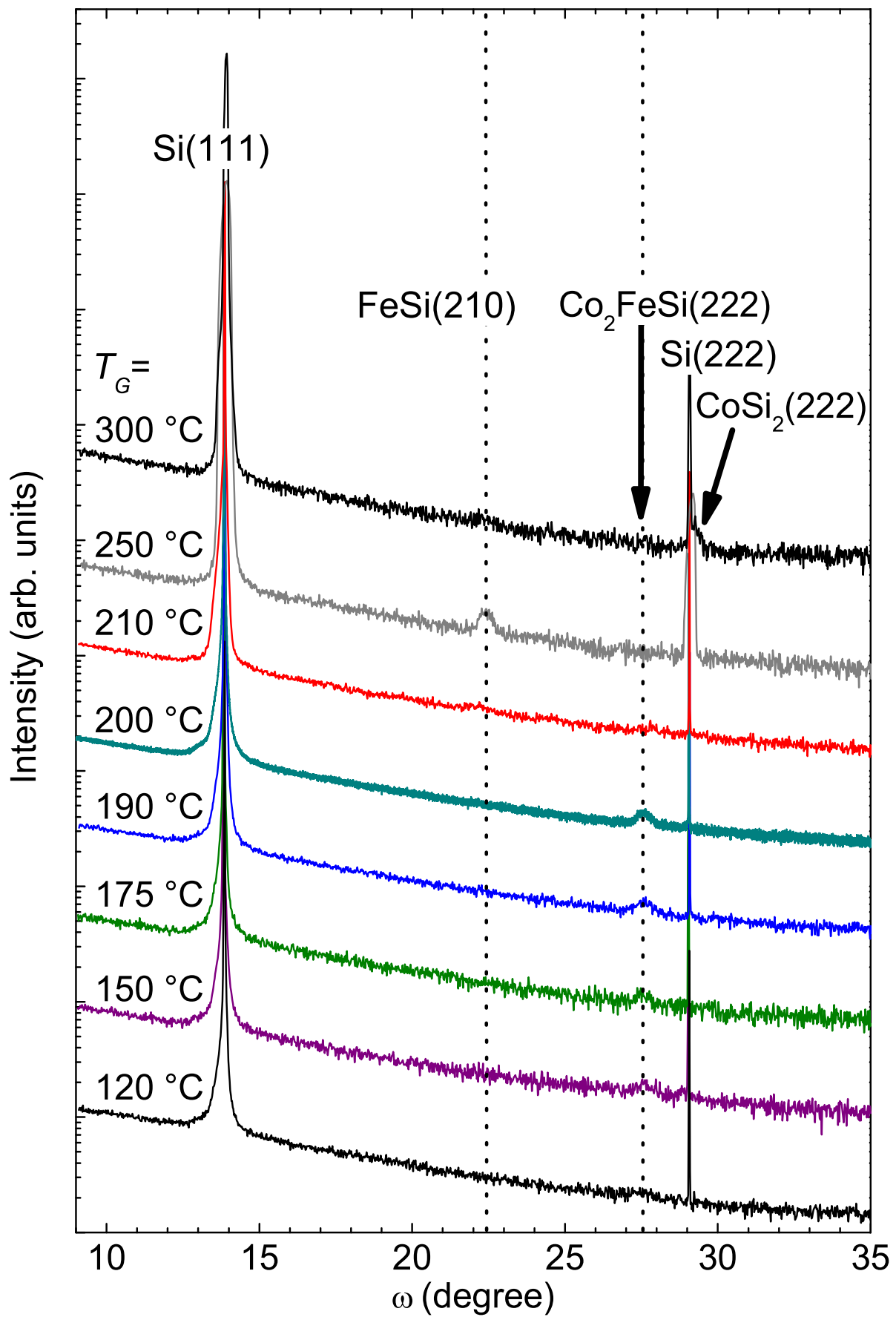


Figure 1 (Article_Zander/fig1.eps)

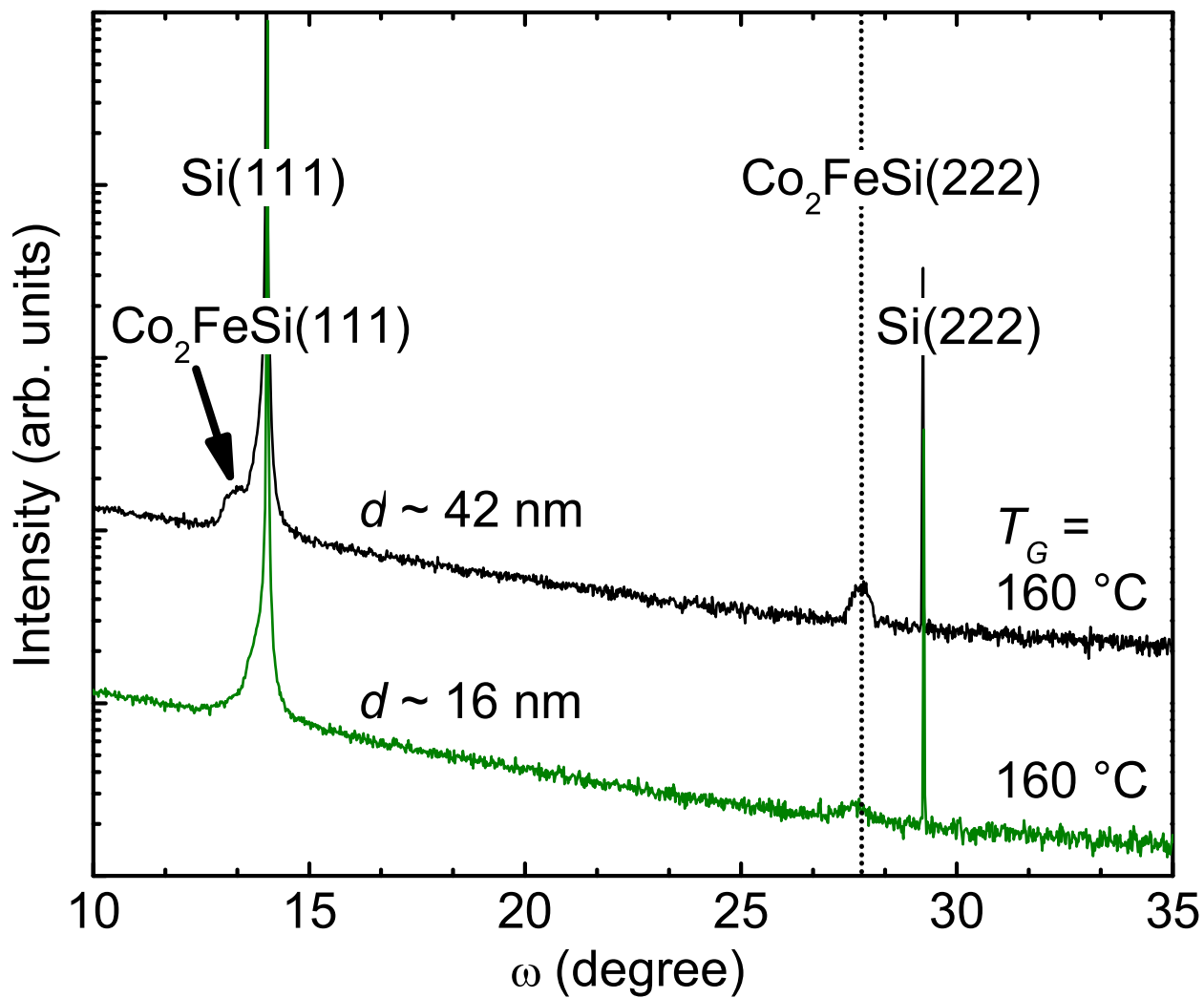


Figure 2 (Article_Zander/fig2.eps)

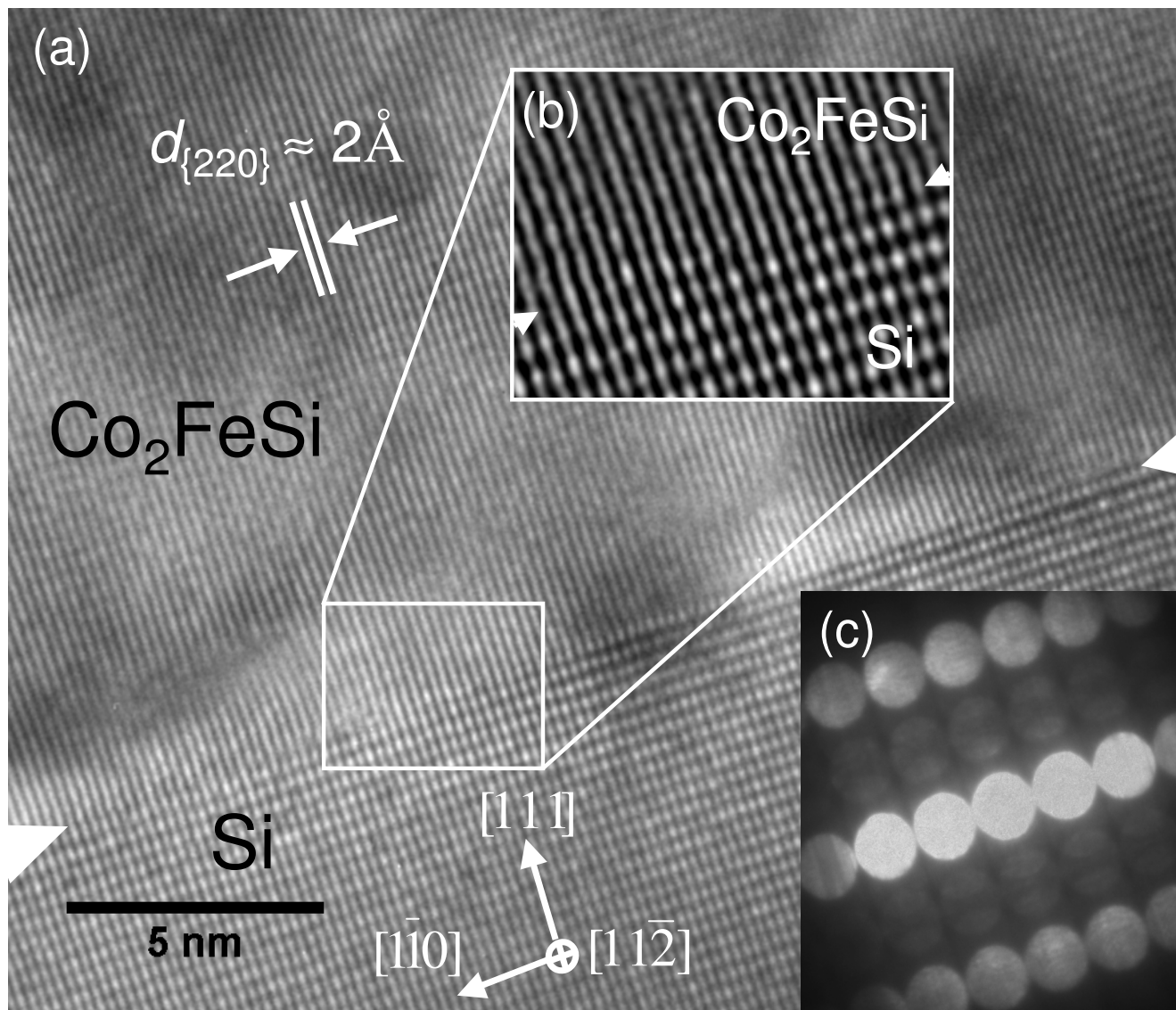


Figure 3 (Article_Zander/fig3.eps)

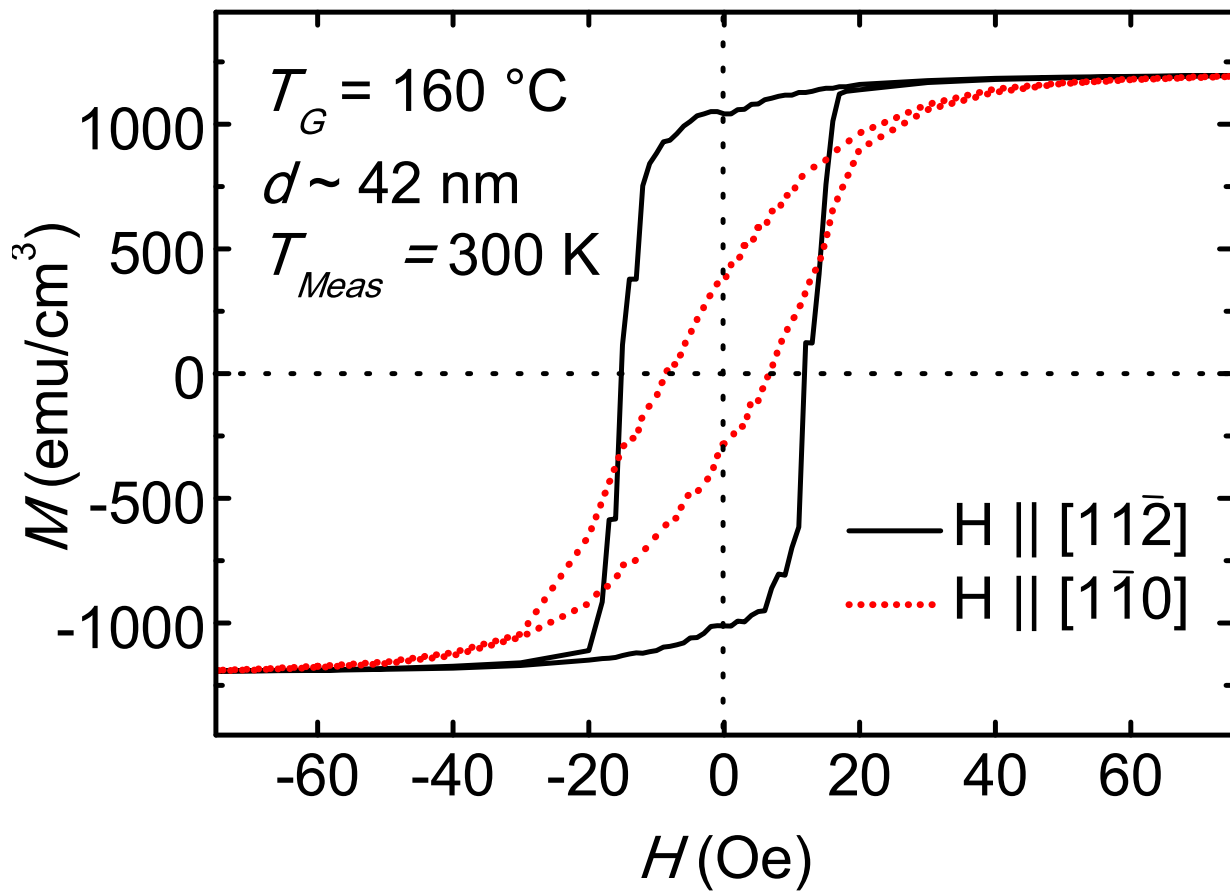


Figure 4 (Article_Zander/fig4.eps)

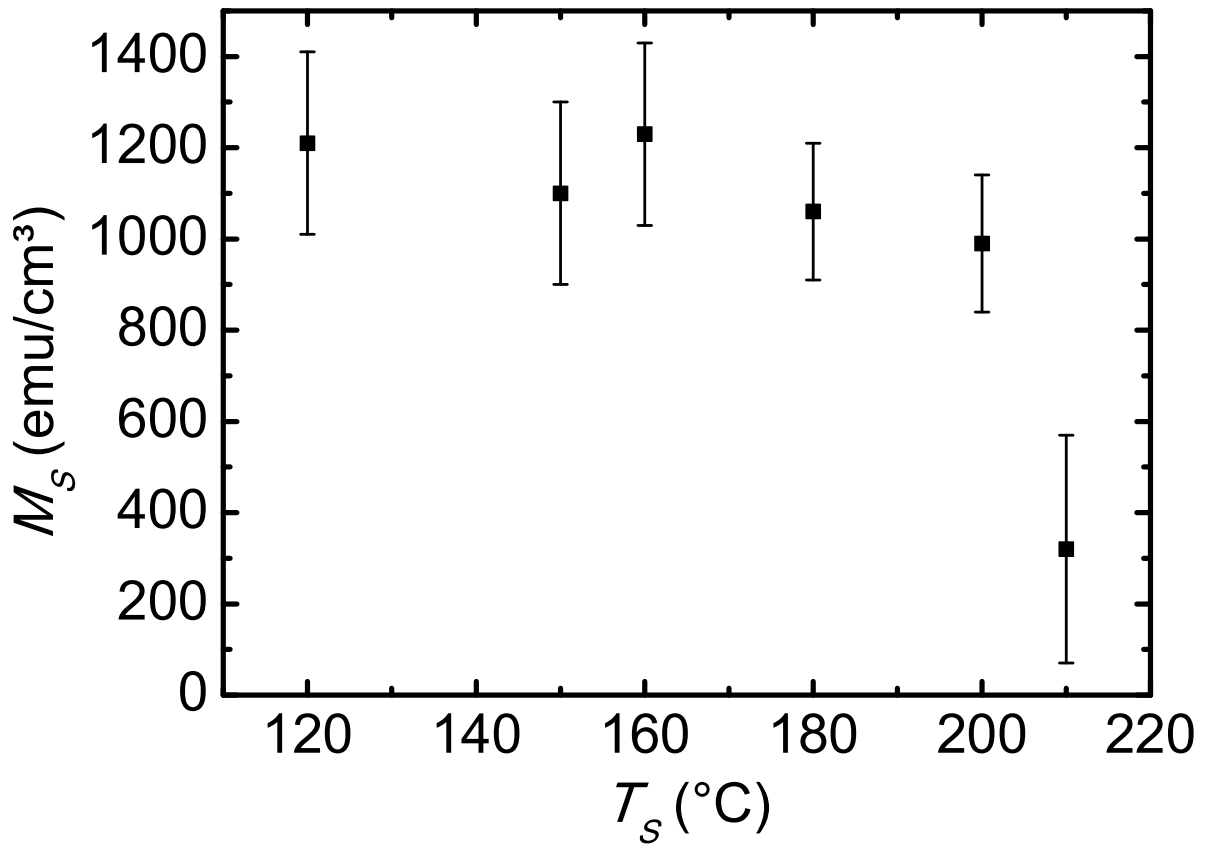


Figure 5 (Article_Zander/fig5.eps)